

DESIGN, SYNTHESIS, AND BIOLOGICAL EVALUATION OF NOVEL 6, 8-DISUBSTITUTED IMIDAZO[1,2-*a*]PYRIDINE DERIVATIVES AS A CDK2 INHIBITORS

Bhargav Bhimani,^{1,3} Ashish Patel,^{2*} Umang Shah,² Afzal Nagani,¹ Vruti Parikh,¹ Harnisha Patel,¹ Hirak Shah,¹ Drashti Shah,² Bhavna Patel,¹ and Nilesh Pandey⁴

¹Department of Pharmaceutical Chemistry, Faculty of Pharmacy, Parul University, Vadodara, Gujarat, India-391760

²Ramanbhai Patel College of Pharmacy, Charotar University of Science and Technology, CHARUSAT Campus, Changa-388421, India.

³Piramal Pharma Limited, Pharmaceutical Special Economic Zone, Ahmedabad, India-382213.

⁴Charotar Institute of Paramedical Science, Charotar University of Science and Technology, CHARUSAT Campus, Changa-388421, India.

Abstract - Imidazo[1,2-*a*]pyridine exerts a notable pharmacological efficiency and has emerged as an integral backbone for the treatment of various cancer. Inhibition of cyclin-dependent kinases has emerged as a potential therapeutic strategy for a variety of cancers. Here, we discuss the synthesis of imidazo[1,2-*a*]pyridine derivatives modified at positions 6 and 8 prepared using Suzuki-Miyaura cross-coupling, Buchwald reaction, and peptide coupling as the main synthetic methods. All synthesized compounds were characterized by spectroscopy techniques after purification and screened for their anti-cancer activity by *in vitro* MTT assays against MCF-T cell line and CDK2 inhibition by kinase inhibition assay. The *in vitro* and kinase inhibition assay revealed that compounds **11ii**, **11iii**, **11xxi**, **11vi**, and **11viii** show potent anti-cancer activity for the treatment of breast cancer. This study demonstrates that substituted imidazo[1,2-*a*]pyridine can be exploited for future cyclin-dependent kinase (CDK2) inhibitor development.

INTRODUCTION

Cancer is distinguished by uncontrolled tumor cell division caused by the abnormal activity of cell cycle proteins. This occurs due to mutations in upstream signaling pathways or genetic lesions in genes encoding cell cycle proteins.^{1,2} It is the second utmost significant reason for death around the globe.³ The World Health Organization (WHO) claims that around 10 million people died in 2020 from various types of cancer, and the figure is predicted to rise to almost 13.1 million by 2030. According to studies, cancer prevalence has risen dramatically, with over 3.0 lakh new cases of malignant tumors detected each year among children aged 0 to 19, with cancer being the leading cause of mortality among children.⁴⁻⁶ The global cancer burden is significant and increasing day by day (Figure 1).⁷

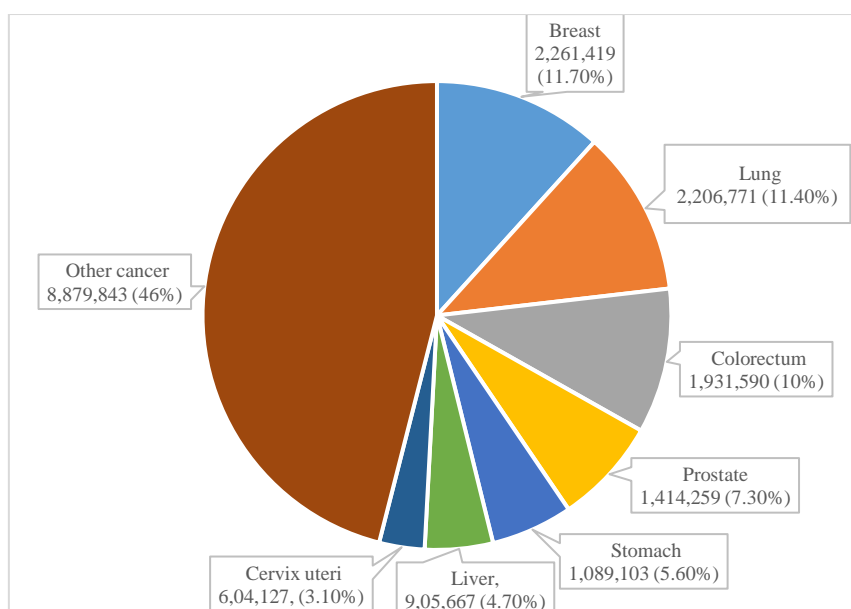


Figure 1. Estimated number of new cases of cancer in 2020, worldwide

Many pieces of data suggested that inhibiting cyclin-dependent kinases (CDKs) could play a crucial role in cancer suppression.⁸⁻¹¹ CDKs have become a potential target for cancer therapy due to their frequent misregulation in tumor cells.¹² Human cells have a total of 20 CDKs (1–20) and 29 cyclins. CDKs are protein-serine/threonine kinases that are members of the CMGC family (cyclin-dependent protein kinases, mitogen-activated protein kinases, glycogen synthase kinases, and CDK-like kinases). As their name implies, CDKs are activated by cyclins, which are proteins that interact with CDKs. After the formation of a CDK-cyclin complex, the CDK activation region is phosphorylated at a conserved threonine residue by CDK7, allowing full expression of CDK-cyclin enzyme activity.^{13,14} However, phosphorylation regulates CDKs, which are necessary for cell growth, cell division, DNA replication, as well as chromosome

separation. Besides, CDK has low kinase activity without cyclin, and the cyclin-CDK complex is the only active kinase.^{9,15} Moreover, aberrant CDKs activity induces spontaneous proliferation, genomic instability, and chromosomal instability, linked to cancer molecular pathogenesis.¹⁶ CDK levels are relatively consistent throughout the cell cycle, while the actions of the cell cycle group of CDKs are regulated by cyclin proteins, whose levels fluctuate over the cell cycle.¹⁷

CDKs are classified into subfamilies based on evolutionary relationships and regulate cell cycles (CDKs 1-6, 11, and 14-18) and transcription. (CDKs 7-13, 19, and 20).¹⁸ Among all, CDK2 is essential for cell cycle progression, cell differentiation, apoptosis, DNA synthesis, G1-S transition, and modulation of G2 progression. Moreover, the cytoplasm, centrosome, nucleus, Cajal bodies, plasma membrane, and endosome all contain CDK2. CDK2 is also known as cell division protein kinase 2, p33 protein kinase, or DKN2.¹⁹⁻²¹ However, hyperactivation of CDK2 and overexpression of cyclins A and E is a critical oncogenic process in human cancers, particularly in breast cancer, ovarian and endometrial carcinomas, lung, thyroid carcinoma, melanoma, and osteosarcoma.^{22,23} Besides, CDK2 is over-expressed in human tumors whereas less expressed in normal tissues, and inhibition of CDK2 also provides a therapeutic benefit to degenerate potential CDK4/6 inhibitor resistance. Thus, selective CDK2 inhibitors serves as a potential and beneficial target against human tumors for the development of anticancer agents.^{2,24}

Moreover, CDK inhibition was seen in several heterocyclic scaffolds, with the purine scaffold being the most potent inhibitor of CDK2. Although, a selective CDK2 inhibitor is yet to be discovered. Roscovitine,²⁵ Dinaciclib,²⁶ Milciclib,²⁷ Roniciclib,²⁸ R547,²⁹ AZD5438,³⁰ TG02,³¹ SNS032,³² BS-194,³³ AT7519,³⁴⁻³⁶ PNU 292137,³⁷ AZ703,³⁸ and other CDK2 inhibitors have recently been tested in preclinical and clinical trials as anticancer medicines. (Figure 2) Using bioisosterism as a rational tool, AstraZeneca developed a novel imidazo[1,2-*a*]pyridine scaffold bearing purine moiety as potent and selective CDK2 inhibitors as anticancer agents. Due to their biological properties, nitrogen-containing heterocyclic compounds, imidazo[1,2-*a*]pyridine (IP), are considered privileged structures.³⁹ The IP cores are recognized as a “drug prejudice” scaffold.⁴⁰ It has been widely exploited in medicinal chemistry due to its broad pharmacological activity spectrum, making it a promising drug candidate for anticancer therapy in smaller toxic and equally effective doses.⁴¹⁻⁴⁴

The present work describes the synthesis of novel 6, 8 di-substituted imidazo[1,2-*a*]pyridine analogues with CDK2 inhibitory action against breast cancer using MCF-7 cell line. All designed compounds were synthesized and screened for their CDK2 inhibition activity by in vitro assay and anti-cancer activity by MTT assay using MCF-7 breast cancer cell line.

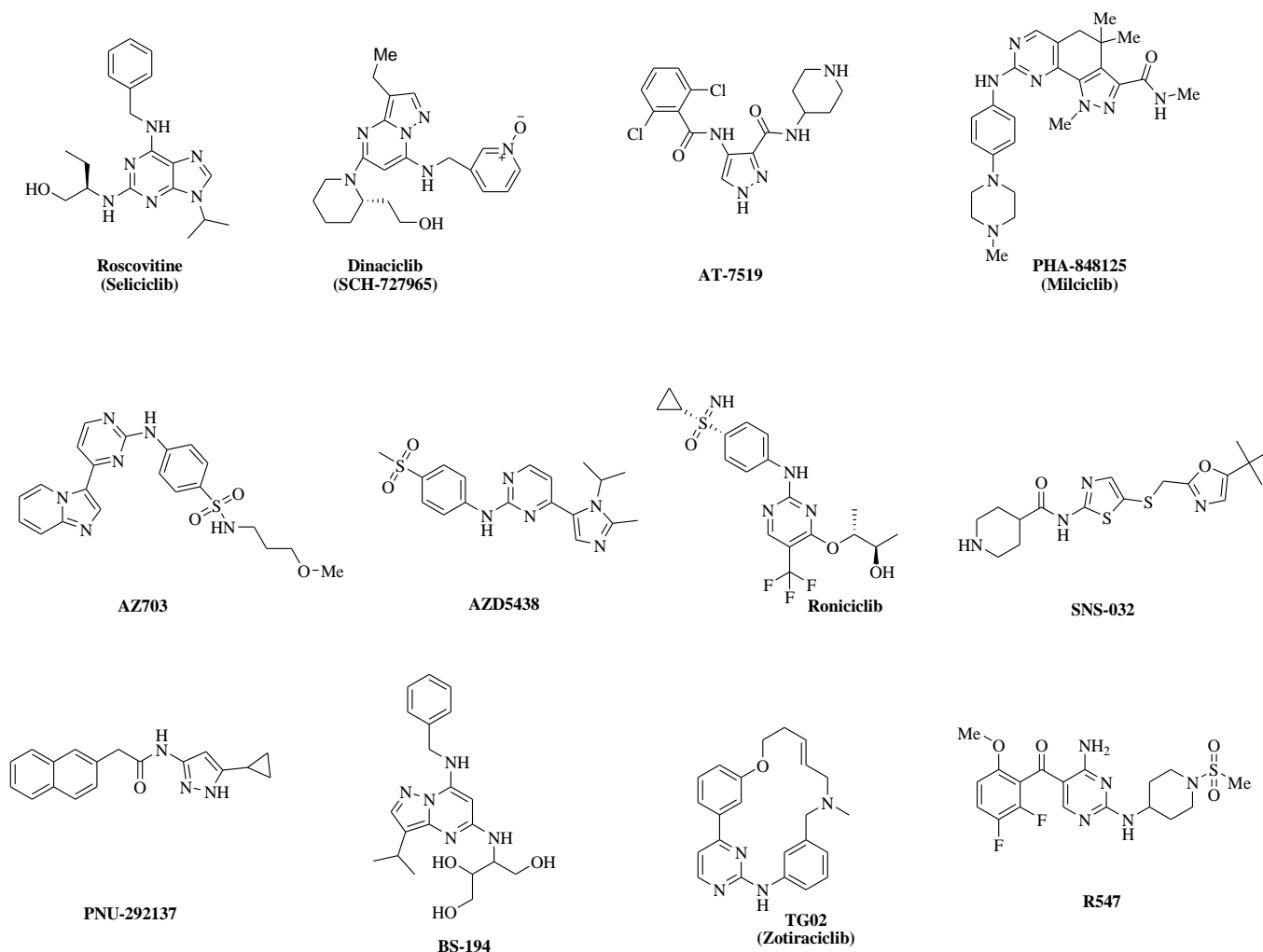


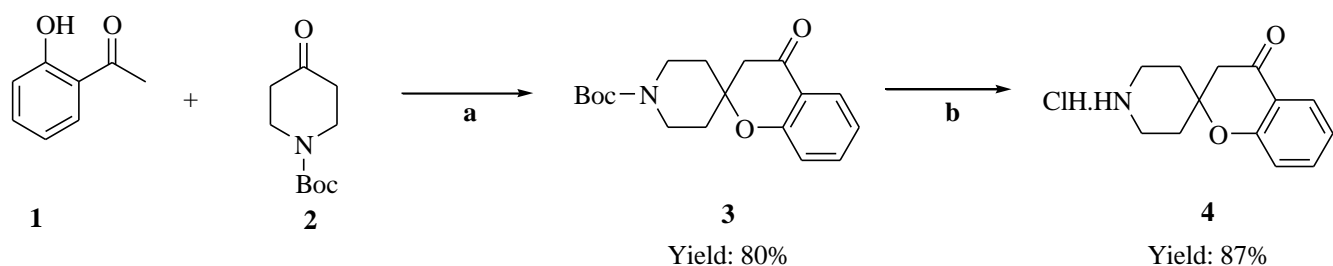
Figure 2. CDK2 inhibitor drugs under preclinical and clinical evaluation

RESULT AND DISCUSSION

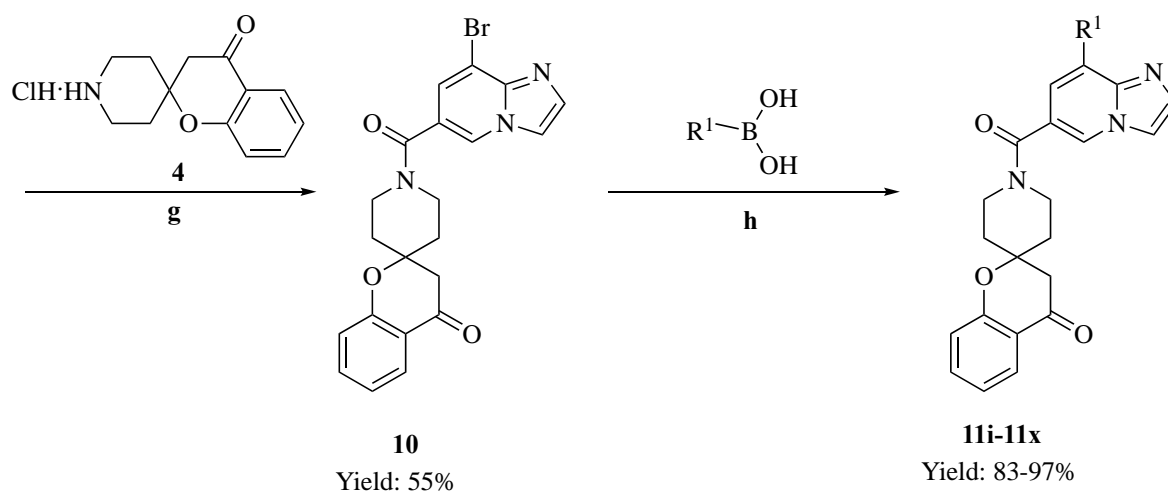
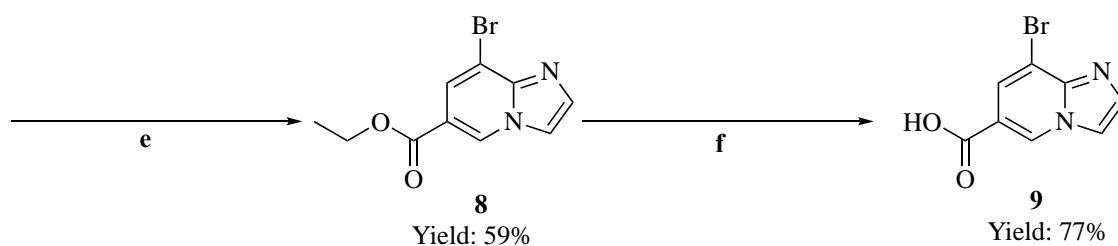
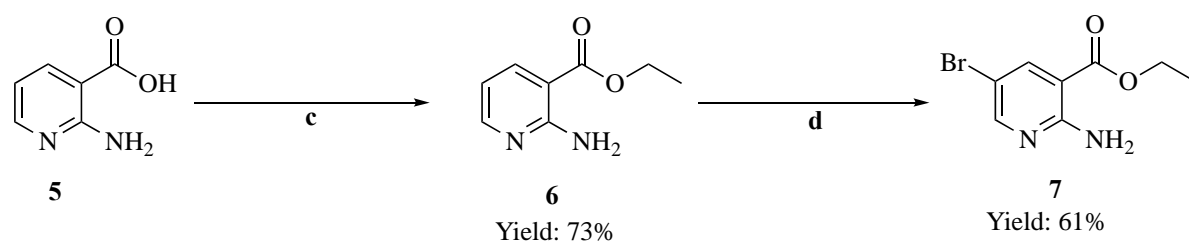
Chemistry

Scheme 1 demonstrates the synthetic pathway of 1-(6-substituted-imidazo[1,2-*a*]pyridine-8-carbonyl)spiro[chromane-2,4'-piperidin]-4-one (**11i-11x**). In the first step, 2-hydroxyacetophenone was treated with Boc protected piperidin-4-one in the presence of pyrrolidine as a base and ethanol as a solvent under reflux conditions for 16 h to obtain intermediate **3** with 80% yield. Furthermore, intermediate **3** undergo a deprotection reaction in presence of HCl in dioxane and DCM as a solvent under mild reaction condition to afford intermediate **4** with 81% yield. (Scheme 1A)

Moreover, as per Scheme 1B, 2-aminonicotinic acid **5** undergoes esterification in the presence of H₂SO₄ as an acid catalyst and ethanol as a solvent under reflux condition for 16 h to afford ester derivative as an intermediate **6** with 73% yield. However, intermediate **6** further reacts with *N*-bromosuccinimide (NBS) using THF as a polar aprotic solvent at 0-25 °C for 8 h to afford intermediate **7** with 61% yield. These intermediate **7** undergoes a cyclization reaction with 2-chloroacetaldehyde and NaHCO₃ as a base in the



Scheme 1A. Synthetic route for intermediate (4). Reagents and conditions: **a)** EtOH, pyrrolidine, reflux, 16 h; **b)** 4M HCl in dioxane, DCM, 0 °C-rt, 3 h.

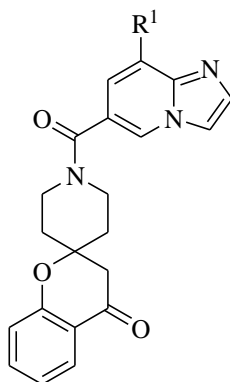


Scheme 1B. Synthetic route for final compounds (**11i-11x**). Reagents and conditions: **c)** EtOH, H₂SO₄, reflux, 16 h; **d)** NBS, THF, 0-25 °C, 8 h; **e)** 2-chloroacetaldehyde, NaHCO₃, EtOH, reflux, 16 h; **f)** LiOH·H₂O, THF, EtOH, H₂O, rt, 2 h; **g)** HATU, DIPEA, DMF, 0 °C-rt, 2 h; **h)** PdCl₂(dppf), DCM, Na₂CO₃, dioxane, reflux, 1 h.

presence of ethanol for 16 h under reflux conditions to give intermediate **8** (yield 59%) which further undergoes a hydrolysis reaction with lithium hydroxide (LiOH·H₂O) using THF, EtOH, and H₂O as a solvent at room temperature for 2 h to obtain intermediate **9** with 77% yield. The intermediate **9** condenses with intermediate **4** using HATU as a catalyst and DIPEA as a strong base using DMF as a solvent under ambient temperature to afford intermediate **10** with 55% yield. Finally, the intermediate **10** undergoes Suzuki coupling reaction with arylboronic acid using PdCl₂(dppf)·DCM complex and Na₂CO₃ base in dioxane solvent under reflux conditions to obtain final imidazo[1,2-*a*]pyridine derivatives (**11i-11x**) with the yield range 83-97%. All the synthesized compounds were characterized by IR, Mass, ¹H-NMR, and ¹³C-NMR spectroscopy.

***In vitro* assay for cytotoxic activity (MTT assay) and CDK2 enzymatic assay**

All 10 compounds were screened for *in vitro* CDK2 inhibitory ADP-Glo™ kinase assay and cytotoxicity activity using MTT assay on the breast cancer cell line (MCF-7). The IC₅₀ values were calculated using the plotted nonlinear graph of percent cell inhibition vs. log concentration in Graphpad Prism software (ver.7). The cytotoxicity was expressed as the mean IC₅₀ of the triplicate values. The results obtained were compared with the standard drugs doxorubicin, 5-fluorouracil, and CDK2 inhibitor. The IC₅₀ values of selected derivatives were in the range of 24.28-157.6 μM for MTT assay and 1.14-72.32 μM for CDK2 enzymatic assay. According to the cytotoxicity results, compounds **11ii**, **11iii**, **11vi**, and **11vii** were found to be more potent. Which were significantly higher as compared with the IC₅₀ values of doxorubicin (81.24 μM) and 5-fluorouracil (99.89). While the rest of the derivatives showed less toxicity against the breast cancer cells (Table 1). However, CDK2 enzymatic assay state that aryloxy/alkoxy group like phenoxy, *o/m/p*-methoxy, 3-ethoxy, and 4-isopropoxy substituted phenyl ring attachment to imidazo[1,2-*a*]pyridine scaffolds by Suzuki cross-coupling reaction increase CDK2 inhibition (Table 1). Whereas, the electron-withdrawing group on the phenyl ring as R¹ (6th position) of imidazo[1,2-*a*]pyridine does not much affect to CDK2 inhibitory activity except in the difluoro/trifluoro group. However, for heteroaryl substitution at the 8th position of imidazo[1,2-*a*]pyridine, unsubstituted/substituted pyridine ring is the best for the development of potent CDK2 inhibitor (**11ii**, **11iii**, **11vi**) for breast cancer treatment. The results in terms of CDK2 inhibition and IC₅₀ for all compounds (**11i-11x**) have been given in Table 1.

Table 1. Results of IC₅₀ values of compounds (**11i-11x**) against CDK2 and MCF-7 cell line at 10 μM

Compound No	R ¹	IC ₅₀ (μM) ^a	
		(MCF-7)	(CDK2)
11i	phenyl	114.9	42.34
11ii	2-methylpyridine	50.04	13.67
11iii	pyridine	36.42	14.45
11iv	4-phenoxyphenyl	109.7	35.45
11v	pyrimidine	56.45	22.43
11vi	2-trifluoromethylpyridine	33.45	8.89
11vii	4-benzyloxyphenyl	24.28	1.14
11viii	4-fluorophenyl	63.38	35.23
11ix	3-cyanophenyl	48.05	22.18
11x	4-chlorophenyl	157.6	72.32
CDK2 inhibitor		NA	0.14
Doxorubicin		81.24	NA
5-Fluorouracil		99.89	NA

CONCLUSION

To summarize, in this study, a series of imidazo[1,2-*a*]pyridine derivatives (**11i-11x**) were designed, synthesized, and tested for CDK2 inhibition to learn more about their potential application as anti-cancer agents. Surprisingly, the CDK2 inhibitory activities of these compounds revealed some extremely potent CDK2 inhibitors. The most active compound 1-(6-(4-phenoxyphenyl)imidazo[1,2-*a*]pyridine-8-carbonyl)spiro[chromane-2,4'-piperidin]-4-one (**11vii**) showed maximum CDK2 inhibition (IC₅₀ = 1.14 μM). Particularly, our findings indicated the requirement of a phenoxy group attached to imidazo[1,2-*a*]pyridine ring including a hydrophobic heteroaryl chromane-piperidine spirocyclic ring through amide linkage (**11vii**) for potential CDK2 inhibition. Moreover, unsubstituted/substituted pyridine attachment

from among all substituted heterocycles to imidazo[1,2-*a*]pyridine scaffolds such as compound **11ii** (IC₅₀ = 13.67 μM) and **11iii** (14.45 μM) was found to be potent CDK2 inhibitor. Besides this, the test compounds' in-silico pharmacokinetic properties predicted drug-like properties for potential oral use as anti-cancer agents. Thus, compound **11vii** shows higher potency against CDK2 making it a promising candidate for further research in the development of novel anti-cancer agents.

EXPERIMENTAL

Chemistry

All solvents and reagents used for the synthesis of desired compounds obtained from commercially available sources such as Spectrochem, S.d. Fine, and Sigma-Aldrich were used. Using a Digital Melting Point Apparatus, the melting points of synthesized compounds were determined. The reaction progress was tracked using silica-gel pre-coated TLC plates and UV visualization. The infrared spectra (IR) were taken using BRUKER ALPHA-T in the region of 4000-500 cm⁻¹. ¹H NMR and ¹³C NMR were acquired in CDCl₃ and DMSO-*d*₆ solvents on Bruker Biospin NMR Spectrometer at 400 MHz. Agilent Mass Spectrometer was used to create high-resolution mass spectra. The final compounds were purified using silica gel as an adsorbent in column chromatography.

Preparation of *tert*-Butyl 4-oxo-3,4-dihydro-1*H*-spiro[naphthalene-2,4-piperidine]-1-carboxylate (**3**)

In a 500 mL four-neck round bottom flask with condenser under a nitrogen atmosphere; 1-(2-hydroxyphenyl)ethanone (**1**) (15 g, 0.1102 mol) and *tert*-butyl 4-oxopiperidine-1-carboxylate (**2**) (21.94 g, 0.1102 mol) were dissolved in MeOH (36%) and pyrrolidone (220 mL) was added at room temperature. The reaction mixture was stirred and refluxed for 16 h. The progress of the reaction was monitored by TLC and LCMS. After completion, the reaction mixture was concentrated under reduced pressure and extracted with EtOAc. The collected organic layer was washed with brine, dried over sodium sulphate, and concentrated under reduced pressure to afford crude which was purified using silica gel (100-200 mesh size) column chromatography. The pure *tert*-butyl 4-oxo-3,4-dihydro-1*H*-spiro[naphthalene-2,4-piperidine]-1-carboxylate (**3**) was eluted in 6-8% EtOAc in hexane as a colorless liquid. Yield: 80%; ¹H NMR (400 MHz, DMSO-*d*₆) δ (ppm): 7.752-7.733 (d, *J*=7.6 Hz, 1H), 7.614-7.575 (t, *J*=7.6 Hz, 1H), 7.098- 7.043 (q, *J*=7.6 Hz, 2H), 3.743-3.714 (d, *J*=11.6 Hz, 2H), 3.141 (s, 2H), 2.854 (s, 2H), 1.903-1.868 (d, *J*=14 Hz, 2H), 1.663-1.611 (t, *J*=10.4 Hz, 2H), 1.411 (s, 9H); ESI-MS *m/z*: 318.9 [M⁺1].

Preparation of 1*H*-Spiro[naphthalene-2,4-piperidin]-4(3*H*)-one hydrochloride salt (**4**)

In a 250 mL three-neck round bottom flask with a calcium chloride guard tube under a nitrogen atmosphere; *tert*-butyl 4-oxo-3,4-dihydro-1*H*-spiro[naphthalene-2,4-piperidine]-1-carboxylate (**3**) (20 g, 0.0630 mol) was dissolved in CH₂Cl₂. The reaction mixture was cooled to 0 °C and 4M HCl in dioxane (20 mL) was added dropwise using a dropping funnel. The reaction mixture was stirred at room temperature for 3 h. The

reaction was monitored by thin-layer chromatography (TLC). After the completion, the reaction mixture was concentrated under reduced pressure to afford a crude product which was purified with Et₂O trituration to afford 1*H*-spiro[naphthalene-2,4-piperidin]-4(3*H*)-one hydrochloride salt (**4**) as a creamy white solid. Yield: 81%; ¹H NMR (400 MHz, DMSO-*d*₆) δ (ppm): 9.390 (s, 1H), 9.190 (s, 1H), 7.755-7.732 (dd, *J*=7.6, 1.2 Hz, 1H), 7.634-7.592 (m, 1H), 7.145-7.065 (m, 2H), 3.184-3.063 (m, 4H), 2.903 (s, 2H), 2.116-2.081 (d, *J*=14 Hz, 2H), 1.981-1.905 (m, 2H).

Preparation of Ethyl 2-aminonicotinate (6)

2-Aminonicotinic acid (**5**) (25 g, 0.1811 mol) was dissolved in EtOH (250 mL) and conc. H₂SO₄ (50 mL) was added dropwise using a dropping funnel at room temperature under a nitrogen atmosphere. The resulting mixture was refluxed for 16 h. The reaction was monitored by TLC and LCMS. After completion, the reaction mixture was concentrated under reduced pressure, cooled to 0 °C, neutralized with 2N NaOH, and extracted with EtOAc. The organic layer was washed with brine, dried over sodium sulphate, and evaporated using a rotary evaporator to yield ethyl 2-aminonicotinate (**6**) as a creamy white solid. Yield: 73%; ¹H NMR (400 MHz, DMSO-*d*₆) δ (ppm): 8.206-8.190 (dd, *J*=4.7, 2.0 Hz, 1H), 8.060-8.037 (dd, *J*=7.7, 2.0 Hz, 1H), 7.173 (s, 2H), 6.634- 6.603 (dd, *J*=7.8, 4.7 Hz, 1H), 4.295-4.241 (q, *J*=7.1 Hz, 2H), 1.314-1.278 (t, *J*=7.1 Hz, 3H); ESI-MS *m/z*: 167.17.[M⁺1].

Preparation of Ethyl 2-amino-5-bromonicotinate (7)

Ethyl 2-aminonicotinate (**6**) (22 g, 0.1325 mol) in THF was cooled to 0 °C under a nitrogen atmosphere and *N*-bromosuccinimide (23.58 g, 0.1325 mol) was added portionwise at 0 °C. The reaction mixture was stirred at room temperature for 8 h. The progress of the reaction was monitored by TLC and LCMS. After completion, the reaction mixture was quenched with saturated sodium bicarbonate solution and extracted with EtOAc. The collected organic layer was dried over sodium sulphate and evaporated using a rotary evaporator to yield ethyl 2-amino-5-bromonicotinate (**7**) as a creamy white solid. Yield: 61%; ¹H NMR (400 MHz, DMSO-*d*₆) δ (ppm): 8.288-8.282 (d, *J*=2.7 Hz, 1H), 8.113-8.107 (d, *J*=2.6 Hz, 1H), 7.351 (s, 2H), 4.302-4.249 (m, 2H), 1.323-1.287 (t, *J*=7.1 Hz, 3H); ESI-MS *m/z*: 246.97 [M⁺2].

Preparation of Ethyl 6-bromoimidazo[1,2-*a*]pyridine-8-carboxylate (8)

Ethyl 2-amino-5-bromonicotinate (**7**) (20 g, 0.0816 mol) was dissolved in EtOH (300 mL) and sodium bicarbonate (13.7 g, 0.1632 mol) was added maintaining an inert atmosphere. Chloroacetaldehyde (50% in H₂O) (64 mL, 0.4080 mol) was added dropwise using a dropping funnel, and the reaction mixture was refluxed for 16 h. The reaction was monitored by TLC and LCMS. After completion, the reaction mixture was concentrated under reduced pressure and neutralized with saturated sodium carbonate solution, and extracted with CH₂Cl₂. The organic layer was washed with brine, dried over sodium sulphate, and concentrated under reduced pressure. The crude product was purified using silica gel (100-200 mesh size) column chromatography to afford pure ethyl 6-bromoimidazo[1,2-*a*]pyridine-8-carboxylate (**8**) as a brown

solid. Yield: 59%; ¹H NMR (400 MHz, DMSO-*d*₆) δ (ppm): 9.175-9.170 (d, *J*=2 Hz, 1H), 8.033-8.031 (d, *J*=0.8 Hz, 1H), 7.850-7.846 (d, *J*=1.6 Hz, 1H), 7.706 (s, 1H), 4.399-4.345 (q, *J*=7.1 Hz, 2H), 1.359-1.324 (t, *J*= 7.1 Hz, 3H); **ESI-MS** *m/z*: 271.7 [M⁺2].

Preparation of 6-Bromoimidazo[1,2-*a*]pyridine-8-carboxylic acid (9)

Ethyl 6-bromoimidazo[1,2-*a*]pyridine-8-carboxylate (**8**) (13 g, 0.0483 mol) was taken in a round bottom flask containing THF (70 mL), EtOH (35 mL), water (35 mL). Lithium hydroxide (10.1 g, 0.2416 mol) was added and the reaction mixture was stirred at room temperature for 2 h. The reaction was monitored by TLC and LCMS. After completion, the organic solvent was concentrated under reduced pressure and neutralized with 5N HCl solution to afford solid precipitates which were filtered through a Buchner funnel and dried under vacuum to afford 6-bromoimidazo[1,2-*a*]pyridine-8-carboxylic acid (**9**) as a brown solid. Yield: 77%; ¹H NMR (400 MHz, DMSO-*d*₆) δ (ppm): 9.390 (s, 1H), 8.245 (s, 2H), 7.982 (s, 1H); **ESI-MS** *m/z*: 243.5 [M⁺2].

Preparation of 1-(6-Bromoimidazo[1,2-*a*]pyridine-8-carbonyl)-1*H*-spiro[naphthalene-2,4-piperidin]-4(3*H*)-one (10)

Under nitrogen atmosphere, 6-bromoimidazo[1,2-*a*]pyridine-8-carboxylic acid (**9**) (9 g, 0.0373 mol) in DMF (90 mL) was cooled to 0 °C and HATU (17 g, 0.0447 mol) was added. The reaction mixture was stirred at 0 °C for 20 min. 1*H*-Spiro[naphthalene-2,4-piperidin]-4(3*H*)-one hydrochloride salt (10.4 g, 0.0410 mol) was added followed by *N,N*-diisopropylethylamine (24 g, 0.1865 mol) at 0 °C and the reaction mixture was stirred at room temperature for 2 h. The reaction was monitored by TLC and LCMS. After completion, the reaction mixture was poured into ice-cold water to afford solid precipitates which were filtered through the Buchner funnel and dried under a vacuum. The crude 1-(6-bromoimidazo[1,2-*a*]pyridine-8-carbonyl)-1*H*-spiro[naphthalene-2,4-piperidin]-4(3*H*)-one (**10**) obtained was then purified by silica gel (100-200 mesh size) column chromatography. Yield: 55%; ¹H NMR (400 MHz, DMSO-*d*₆) δ (ppm): 8.995 (s, 1H), 8.007 (s, 1H), 7.751-7.731 (d, *J*=8 Hz, 1H), 7.665 (s, 1H), 7.626-7.587 (t, *J*=7.6 Hz, 1H), 7.427 (s, 1H), 7.134-7.113 (d, *J*=8.4 Hz, 1H), 7.084-7.047 (t, *J*= 7.2 Hz, 1H), 4.330-4.299 (d, *J*=12.4 Hz, 1H), 3.354-3.207 (m, 3H), 2.887 (s, 2H), 2.080-2.008 (t, *J*=14 Hz, 2H), 1.832-1.765 (t, *J*=14.4 Hz, 3H); **ESI-MS** *m/z*: 442.6 [M⁺2].

General Procedure for the Synthesis of 1-(6-Substituted-imidazo[1,2-*a*]pyridine-8-carbonyl)spiro[chromane-2,4'-piperidin]-4-one derivatives (11i-11x)

Under an inert atmosphere, 1-(6-bromoimidazo[1,2-*a*]pyridine-8-carbonyl)-1*H*-spiro[naphthalene-2,4-piperidin]-4(3*H*)-one (**10**) (0.0003 mol) was dissolved in dioxane (6 mL) and water (2 mL). Substituted phenylboronic acid (0.00036 mol) and Na₂CO₃ (0.0009 mol) were added. The reaction mixture was degassed with argon for 5 min. PdCl₂(dppf) (0.00003 mol) was added and degassed for 2 min. The reaction mixture was heated at 100 °C for 1 h. The progress of the reaction was monitored by TLC and LCMS. After

completion, the reaction mixture was diluted with water and extracted with EtOAc. The organic layer was washed with brine and dried over sodium sulphate and evaporated using a rotary evaporator. The crude residue obtained was purified using combi-flash chromatography to afford pure final derivatives (**11i-11x**).

1-(6-Phenylimidazo[1,2-*a*]pyridine-8-carbonyl)spiro[chromane-2,4'-piperidin]-4-one (11i)

Yield: 90%; Mp 136-138 °C; IR (KBr, cm⁻¹): 3059.05 (C-H, Aromatic), 2923.13 (C-H, Aliphatic), 1688.48 (C=O, Ketone), 1634.48 (C=O, Amide), 1576.93, 1370.78 (C=C, Aromatic), 1221.29 (C-N, Str), 1025.26 (C-O, Str); ¹H NMR (400 MHz, DMSO-*d*₆) δ (ppm): 9.002 (s, 1H), 8.041-8.019 (d, *J*=8.8 Hz, 1H), 7.732 (s, 3H), 7.656-7.576 (m, 3H), 7.535-7.50 (t, *J*=6.8 Hz, 2H), 7.438-7.402 (t, *J*=7.2 Hz, 1H), 7.127-7.036 (m, 2H), 4.387-4.337 (d, *J*=12 Hz, 1H), 3.329 (m, 3H), 2.884 (s, 3H), 2.092-2.058 (d, *J*=13.6 Hz, 1H), 1.849-1.817 (t, *J*=12.8 Hz, 3H); ¹³C NMR (100 MHz, DMSO-*d*₆) δ (ppm): 33.42, 34.34, 37.33, 42.82, 47.23, 78.68, 114.82, 118.86, 120.81, 121.64, 122.89, 125.10, 125.28, 126.14, 126.34, 127.04, 128.37, 129.62, 134.48, 134.53, 136.61, 137.03, 140.93, 159.01, 165.10, 191.85; ESI-MS *m/z*: 438.8

[M⁺1].

1-(6-(2-Methylpyridin-4-yl)imidazo[1,2-*a*]pyridine-8-carbonyl)spiro[chromane-2,4'-piperidin]-4-one (11ii)

Yield: 90%; Mp 130-132 °C; IR (KBr, cm⁻¹): 3077.77 (C-H, Aromatic), 2921.14 (C-H, Aliphatic), 1687.87 (C=O, Ketone), 1633.52 (C=O, Amide), 1555.85, 1371.83 (C=C, Aromatic), 1214.96 (C-N, Str), 1025.73 (C-O, Str); ¹H NMR (400 MHz, DMSO-*d*₆) δ (ppm): 9.323 (s, 1H), 8.555-8.542 (d, *J*=5.2 Hz, 1H), 8.071 (s, 1H), 7.741 (s, 2H), 7.702 (s, 2H), 7.626-7.591 (t, *J*=8.4 Hz, 3H), 7.138-7.047 (m, 2H), 4.380-4.347 (d, *J*=13.2 Hz, 1H), 3.422-3.294 (m, 3H), 2.900 (s, 2H), 2.562 (s, 3H), 2.110-2.075 (d, *J*=14.4 Hz, 1H), 1.854-1.790 (t, *J*=15.2 Hz, 3H); ¹³C NMR (100 MHz, DMSO-*d*₆) δ (ppm): 24.62, 33.46, 34.39, 37.35, 42.82, 47.23, 78.66, 115.14, 118.45, 118.86, 120.59, 120.82, 121.67, 122.02, 122.40, 126.36, 126.40, 126.53, 134.91, 137.05, 141.28, 144.06, 150.15, 159.02, 159.26, 164.94, 191.83; ESI-MS *m/z*: 453.4 [M⁺1].

1-(6-(Pyridin-4-yl)imidazo[1,2-*a*]pyridine-8-carbonyl)spiro[chromane-2,4'-piperidin]-4-one (11iii)

Yield: 89%; Mp 218-220 °C; IR (KBr, cm⁻¹): 3121.42 (C-H, Aromatic), 2921.78 (C-H, Aliphatic), 1686.25 (C=O, Ketone), 1628.00 (C=O, Amide), 1221.22 (C-N, Str), 1023.66 (C-O, Str); ¹H NMR (400 MHz, DMSO-*d*₆) δ (ppm): 9.254 (s, 1H), 8.699-8.686 (d, *J*=5.2 Hz, 2H), 8.081 (s, 1H), 7.819-7.805 (d, *J*=5.6 Hz, 2H), 7.759-7.708 (m, 2H), 7.625-7.541 (m, 2H), 7.138-7.046 (m, 2H), 4.380-4.347 (d, *J*=13.2 Hz, 1H), 3.389-3.264 (m, 3H), 2.900 (s, 2H), 2.108-2.074 (d, *J*=13.6 Hz, 1H), 1.854-1.789 (t, *J*=14.4 Hz, 3H); ¹³C NMR (100 MHz, DMSO-*d*₆) δ (ppm): 33.47, 34.37, 37.36, 42.83, 47.24, 78.67, 115.19, 118.86, 120.82, 121.38, 121.67, 121.92, 122.22, 126.36, 126.45, 126.67, 134.95, 137.05, 141.29, 143.89, 150.84, 159.02, 164.91, 191.83; ESI-MS *m/z*: 439.4 [M⁺1].

1-(6-(4-Phenoxyphenyl)imidazo[1,2-*a*]pyridine-8-carbonyl)spiro[chromane-2,4'-piperidin]-4-one (11iv)

Yield: 91%, Mp 119-121 °C; IR (KBr, cm⁻¹): 3069.04 (C-H, Aromatic), 2923.72 (C-H, Aliphatic), 1689.74 (C=O, Ketone), 1635.91 (C=O, Amide), 1372.21 (C=C, Aromatic), 1238.10 (C-N, Str), 1023.87 (C-O, Str); ¹H NMR (400 MHz, DMSO-*d*₆) δ (ppm): 8.990(s, 1H), 8.040-8.021(d, *J*=7.6 Hz, 1H), 7.825-7.731 (m, 3H), 7.660 (s, 1H), 7.614-7.587 (d, *J*=10.8 Hz 2H), 7.470-7.431 (t, *J*=8 Hz 2H), 7.222-7.045 (m, 6H), 4.374-4.341 (d, *J*=13.2 Hz 1H), 3.390-3.309 (m, 3H), 2.895 (s, 2H), 2.098-2.063 (d, *J*=14 Hz, 1H), 1.854-1.786 (t, *J*=14.4 Hz, 3H); ¹³C NMR (100 MHz, DMSO-*d*₆) δ (ppm): 33.46, 34.37, 37.34, 42.83, 47.25, 78.69, 114.79, 117.60, 118.87, 119.45, 119.55, 120.83, 121.66, 122.82, 124.29, 124.54, 124.93, 126.16, 126.36, 128.76, 130.56, 130.65, 131.72, 134.50, 136.64, 137.03, 140.87, 155.80, 157.21, 159.03, 165.13, 191.83; ESI-MS *m/z*: 530.4 [M⁺1].

1-(6-(Pyrimidin-2-yl)imidazo[1,2-*a*]pyridine-8-carbonyl)spiro[chromane-2,4'-piperidin]-4-one (11v)

Yield: 92%; Mp 170-172 °C; IR (KBr, cm⁻¹): 3087.21 (C-H, Aromatic), 2923.23 (C-H, Aliphatic), 1687.89 (C=O, Ketone), 1634.01 (C=O, Amide), 1373.31 (C=C, Aromatic), 1226.03 (C-N, Str), 1027.58 (C-O, Str); ¹H NMR (400 MHz, DMSO-*d*₆) δ (ppm): 9.237-9.205 (m, 3H), 8.077 (s, 1H), 7.780-7.718 (m, 3H), 7.627-7.569 (m, 2H), 7.138-7.047 (m, 2H), 4.376-4.344 (d, *J*=12.8 Hz, 1H), 3.394-3.271 (m, 3H), 2.903 (s, 2H), 2.110-2.076 (d *J*=13.6 Hz, 1H), 1.865-1.778 (t, *J*=9.2 Hz, 3H); ¹³C NMR (100 MHz, DMSO-*d*₆) δ (ppm): 33.51, 34.36, 37.37, 42.83, 47.24, 78.67, 114.30, 115.08, 118.86, 119.13, 120.82, 121.67, 122.03, 126.33, 126.36, 130.49, 134.92, 137.04, 141.08, 155.15, 157.96, 159.01, 164.83, 191.81; ESI-MS *m/z*: 440.3 [M⁺1].

1'-(6-(2-(Trifluoromethyl)pyridin-4-yl)imidazo[1,2-*a*]pyridine-8-carbonyl)spiro[chromane-2,4'-piperidin]-4-one (11vi)

Yield: 83%; Mp 160-162 °C; IR (KBr, cm⁻¹): 2922.70 (C-H, Aliphatic), 1689.03 (C=O, Ketone), 1634.44 (C=O, Amide), 1578.26, 1360.34 (C=C, Aromatic), 1222.90 (C-N, Str), 1025.95 (C-O, Str); ¹H NMR (400 MHz, DMSO-*d*₆) δ (ppm): 9.423 (s, 1H), 8.885-8.872 (d, *J*=5.2 Hz, 1H), 8.336 (s, 1H), 8.164-8.151 (d, *J*=5.2 Hz, 1H), 8.091 (s, 1H), 7.899 (s, 1H), 7.750-7.73 3(d, *J*=6.8 Hz, 2H), 7.629-7.590 (t, *J*=8 Hz, 1H), 7.138-7.048 (m, 2H), 4.383-4.350 (d, *J*=13.2 Hz, 1H), 3.556-3.264 (m, 3H), 2.903 (s, 2H), 2.116-2.081 (d, *J*=14 Hz, 1H), 1.841-1.787 (t, *J*=10.4 Hz, 3H); F NMR: -66.352 (s, 1H); ¹³C NMR (100 MHz, DMSO-*d*₆) δ (ppm): 33.48, 34.41, 37.32, 42.82, 47.23, 78.65, 115.34, 118.20, 118.85, 120.83, 121.03, 121.68, 121.88, 124.67, 126.36, 126.49, 127.70, 135.19, 137.04, 141.37, 146.31, 147.91 (q, *J* = 34 Hz), 151.41, 159.01, 164.69, 191.80; ESI-MS *m/z*: 507.3 [M⁺1].

1'-(6-(4-(Benzyloxy)phenyl)imidazo[1,2-*a*]pyridine-8-carbonyl)spiro[chromane-2,4'-piperidin]-4-one (11vii)

Yield: 97%; Mp 110-112 °C; IR (KBr, cm⁻¹): 3033.70 (C-H, Aromatic), 2922.80 (C-H, Aliphatic), 1689.23 (C=O, Ketone), 1634.26 (C=O, Amide), 1576.32, 1373.68 (C=C, Aromatic), 1221.89 (C-N, Str), 1023.92 (C-O, Str); ¹H NMR (400 MHz, DMSO-*d*₆) δ (ppm): 8.922 (s, 1H), 8.001 (s, 1H), 7.733-7.573 (m, 6H), 7.488-7.470 (d, *J*=7.2 Hz, 2H), 7.428-7.391 (t, *J*=7.2 Hz, 2H), 7.360-7.325 (t, *J*=7.2 Hz, 1H), 7.156-7.029 (m, 4H), 5.175 (s, 2H), 4.359-4.326 (d, *J*=13.2 Hz, 1H), 3.352-3.286 (m, 3H), 2.877 (s, 2H), 2.079-2.044 (d, *J*=14 Hz, 1H), 1.834-1.786 (t, *J*=14 Hz, 3H); ¹³C NMR (100 MHz, DMSO-*d*₆) δ (ppm): 33.47, 34.36, 37.34, 42.83, 47.26, 69.75, 78.69, 114.66, 115.93, 118.86, 120.84, 121.65, 122.85, 124.44, 124.86, 126.08, 126.35, 128.17, 128.23, 128.35, 128.94, 129.12, 134.38, 136.31, 137.02, 137.45, 137.55, 140.82, 158.71, 159.03, 165.20, 191.82; ESI-MS *m/z*: 544.7[M⁺1].

1'-(6-(4-Fluorophenyl)imidazo[1,2-*a*]pyridine-8-carbonyl)spiro[chromane-2,4'-piperidin]-4-one (11viii)

Yield: 88%; Mp 172-174 °C; IR (KBr, cm⁻¹): 3124.25 (C-H, Aromatic), 2924.10 (C-H, Aliphatic), 1687.21 (C=O, Ketone), 1634.20 (C=O, Amide), 1370.47 (C=C, Aromatic), 1257.21 (C-N, Str), 1024.87 (C-O, Str); ¹H NMR (400 MHz, DMSO-*d*₆) δ (ppm): 8.997 (s, 1H), 8.038 (s, 1H), 7.845-7.729 (m, 3H), 7.666 (s, 1H), 7.617-7.588 (d, *J*=11.6 Hz, 2H), 7.389-7.345 (t, *J*=8.8 Hz, 2H), 7.162-7.045 (m, 2H), 4.375-4.341 (d, *J*=13.6 Hz, 1H), 3.388-3.310 (m, 3H), 2.894 (s, 2H), 2.099-2.065 (d, *J*=13.6 Hz, 1H), 1.851-1.786 (t, *J*=14.4 Hz, 3H); ¹³C NMR (100 MHz, DMSO-*d*₆) δ (ppm): 33.47, 34.37, 37.35, 42.83, 47.25, 78.68, 114.64, 114.82, 116.45 (d, *J*=22 Hz), 118.85, 120.83, 121.65, 122.86, 124.21, 125.28, 126.17, 126.35, 127.88, 129.16 (d, *J*=8.0 Hz), 133.14, 133.16, 134.55, 136.95, 137.02, 140.89, 159.03, 162.51 (d, *J*=243 Hz), 165.08, 191.81; F NMR: -114.701 (s, 1H); ESI-MS *m/z*: 456.6 [M⁺1].

3-(8-(4-Oxospiro[chromane-2,4'-piperidine]-1'-carbonyl)imidazo[1,2-*a*]pyridin-6-yl)benzotrile (11ix)

Yield: 84%; Mp 215-217 °C; IR (KBr, cm⁻¹): 3076.67 (C-H, Aromatic), 2922.21 (C-H, Aliphatic), 1687.69 (C=O, Ketone), 1634.68 (C=O, Amide), 1577.80, 1371.28 (C=C, Aromatic), 1226.09 (C-N, Str), 1025.37 (C-O, Str); ¹H NMR (400 MHz, DMSO-*d*₆) δ (ppm): 9.141-9.138 (d, *J*=1.2 Hz, 1H), 8.271 (s, 1H), 8.117-8.098 (d, *J*=7.6 Hz, 1H), 8.037 (s, 1H), 7.888-7.862 (d, *J*=11.2 Hz, 1H), 7.739-7.683 (m, 4H), 7.612-7.577 (t, *J*=7.2 Hz, 1H), 7.124-7.104 (d, *J*=9.2 Hz, 1H), 7.072-7.035 (t, *J*=7.6 Hz, 1H), 4.368-4.335 (d, *J*=13.2 Hz, 1H), 3.413-3.260 (m, 3H), 2.893 (s, 2H), 2.101-2.066 (d, *J*=14 Hz, 1H), 1.852-1.805 (t, *J*=9.6 Hz, 3H); ¹³C NMR (100 MHz, DMSO-*d*₆) δ (ppm): 33.47, 34.38, 37.33, 42.81, 47.22, 78.66, 112.71, 114.99, 118.84, 119.11, 120.81, 121.65, 122.47, 123.12, 126.20, 126.30, 126.34, 130.66, 130.77, 131.74, 131.83, 134.81, 137.02, 137.87, 141.03, 158.99, 164.94, 191.8; ESI-MS *m/z*: 463.6 [M⁺1].

**1'-(6-(4-Chlorophenyl)imidazo[1,2-*a*]pyridine-8-carbonyl)spiro[chromane-2,4'-piperidin]-4-one
(11x)**

Yield: 84%; Mp 212-214 °C; IR (KBr, cm⁻¹): 3075.97 (C-H, Aromatic), 2923.39 (C-H, Aliphatic), 1689.09 (C=O, Ketone), 1633.19 (C=O, Amide), 1578.02, 1370.97 (C=C, Aromatic), 1221.47 (C-N, Str), 1025.47 (C-O, Str); ¹H NMR (400 MHz, DMSO-*d*₆) δ (ppm): 9.048 (s, 1H), 8.046 (s, 1H), 7.795-7.731 (m, 3H), 7.673 (s, 1H), 7.638-7.574 (m, 3H), 7.135-7.044 (m, 2H), 4.375-4.342 (d, *J*=13.2 Hz, 1H), 3.388-3.288 (m, 3H), 2.893 (s, 2H), 2.100-2.066 (d, *J*=13.6 Hz, 1H), 1.852-1.786 (t, *J*=14.8 Hz, 3H); ¹³C NMR (100 MHz, DMSO-*d*₆) δ (ppm): 33.47, 34.37, 37.36, 42.83, 47.25, 78.68, 114.91, 118.86, 120.83, 121.65, 122.64, 123.67, 125.53, 126.25, 126.35, 127.92, 128.83, 129.56, 133.18, 134.63, 135.55, 136.43, 137.02, 140.96, 159.02, 165.04, 191.81; ESI-MS, *m/z*: 472.6 [M⁺1].

BIOLOGICAL EVALUATION

Kinase inhibition assay

The CDK inhibitory activity assay was carried out with the help of the ADP-Glo™ kinase assay kit. In a final buffer of 25 mM HEPES (pH 7.4), 10 mM MgCl₂, 0.01 percent Triton X-100, 100 mL1 BSA, 2.5 mM DTT, the recombinant human CDK2 were incubated with substrates, compounds, and ATP in a 384-well plate with a total volume of 10 L, respectively. The ADP-Glo™ kinase assay was then performed, followed by the addition of 5 L ADP-Glo Reagent to stop the kinase reaction and deplete the unconsumed ATP. After that, the mixture was incubated for 40 min at room temperature, and the luminescence was measured using a plate-reading luminometer. The signal was inversely correlated with the kinase activity and was correlated with the amount of ATP present in the reaction.⁴⁵⁻⁴⁷ The IC₅₀ value was calculated using dose-response curves to determine the concentration of test compounds required to reduce activity by 50%.

***In vitro* MTT assay against cancer cell line (MCF-7)**

MCF-7, a human breast adenocarcinoma cell line was procured from the National Centre for Cell Science, Pune, India. The cells were grown in the vented cell culture flask (Corning, USA) with 25 cm² area using Minimum Essential Medium (MEM) (Thermo Fisher, USA). The MEM was supplemented with Fetal Bovine Serum (FBS) (Thermo Fisher, USA), Antibiotic-Antimycotic solution containing penicillin (100 units/mL), streptomycin (100 µg/mL), and Amphotericin B (0.25 µg/mL) (Thermo Fisher, USA), 1.25 mM HEPES (4-(2-hydroxyethyl)-1-piperazine-1-ethanesulfonic acid) (Thermo Fisher, USA) and 1mM sodium pyruvate (Thermo Fisher, USA). The cell line was incubated at 37 °C with 5% CO₂ supply and 95% humidity.

The cytotoxicity of the imidazo[1,2-*a*]pyridine derivatives⁴⁸ were evaluated using MTT [3-(4,5-dimethylthiazol-2-yl)-2,5-diphenyltetrazolium bromide] assay as per the protocol published in ATCC for their growth inhibitory activity against the breast cancer cell line (MCF-7). Briefly, the cells were seeded

on a 96-well plate with a cell density of 10000 cells/well and incubated for 24 h at 37 °C with 5% CO₂ supply and 95% humidity. The cells were then treated with flavonoid derivatives at concentrations of 10, 20, 40, 60, 80, and 100 mM and allowed to incubate for 24 h. After incubation, the supernatant was discarded and each well is supplied with 25 µL of MTT solution (5 mg/mL in PBS) followed by 3 h of incubation. Again the supernatant is discarded and the formazan complex was dissolved in 100 µL dimethyl sulfoxide (DMSO). The absorbance of the dissolved complex was recorded at 570 nm on an ELISA plate reader (Molecular Devices, USA). Doxorubicin, an anti-cancer antibiotic containing an anthracycline ring system, and 5-fluorouracil (5-FU), a pyrimidine analogue were considered reference drugs. The IC₅₀ values were measured using graph pad prism software (ver.7), using the plotted nonlinear graph of percent cell inhibition vs log concentration.^{49,50} The percent inhibition of cell growth was determined as per the formula below.

$$\% \text{ Cell Viability} = (A_T / A_U) \times 100$$

Where, A_T = Absorbance of Treated Cells (Drug)

A_U = Absorbance of Untreated Cells

$$\% \text{ Cell Inhibition} = 100 - \% \text{ Cell Viability}$$

CONSENT FOR PUBLICATION

Not applicable.

CONFLICT ON INTEREST

The authors declare no conflict of interest, financial or otherwise.

ACKNOWLEDGEMENTS

Authors thanks Parul Institute of Pharmacy and Ramanbhai Patel College of Pharmacy, Charotar University of Science and Technology for providing necessary facilities for research work.

REFERENCES AND NOTES

1. M. Malumbres and M. Barbacid, *Nat. Rev. Cancer*, 2009, **9**, 153.
2. T. Otto and P. Sicinski, *Nat. Rev. Cancer*, 2017, **17**, 93.
3. Centre for Disease Control and Prevention. <https://www.cdc.gov/cancer/dcpc/research/update-on-cancer-deaths/index.htm> (Accessed 21 March 2022).
4. WHO global cancer report. https://www.who.int/health-topics/cancer#tab=tab_1 (Accessed 11 March 2022).
5. Y. Wan, Y. Li, C. Yan, M. Yan, and Z. Tang, *Eur. J. Med. Chem.*, 2019, **183**, 111691.

6. global-initiative-for-childhood-cancer <https://www.who.int/publications/m/item/global-initiative-for-childhood-cancer> (Accessed 12 March 2022).
7. International Agency for Research on Cancer. <https://gco.iarc.fr/> (Accessed 8 March 2022).
8. D. Ahmed and M. Sharma, *Int. J. Endocrinol.*, 2011, **2011**, 530274.
9. W. Cheng, Z. Yang, S. Wang, Y. Li, H. Wei, X. Tian, and Q. Kan, *Eur. J. Med. Chem.*, 2019, **164**, 615.
10. Z. Liu, C. Cheng, X. Luo, Q. Xia, Y. Zhang, X. Long, Q. Jiang, and W. Fang, *BMC Cancer*, 2016, **16**, 273.
11. Q. S. Zhang, Y. G. Liao, Z. Ji, Y. Gu, H. S. Jiang, Z. S. Xie, S. Y. Pan, and Y. F. Hu, *Exp. Ther. Med.*, 2016, **12**, 2594.
12. A. Fiset, E. Xu, S. Bergeron, A. Marette, G. Pelletier, K. A. Siminovitch, M. Olivier, N. Beauchemin, and R. L. Faure, *Cellulose*, 2011, **23**, 911.
13. M. Malumbres, *Genome Biol.*, 2014, **15**, 122.
14. G. Manning, D. B. Whyte, R. Martinez, T. Hunter, and S. Sudarsanam, *Science*, 2002, **298**, 1912.
15. A. I. Daa and M. E. Amira, *Eur. J. Med. Chem.*, 2010, **45**, 1158.
16. M. B. Kastan and J. Bartek, *Nature*, 2004, **432**, 316.
17. C. J. Sherr, *Science*, 1996, **274**, 1672.
18. S. Lapenna and A. Giordano, *Nat. Rev. Drug Discov.*, 2009, **8**, 547.
19. L. de Boer, V. Oakes, H. Beamish, N. Giles, F. Stevens, M. Somodevilla-Torres, C. DeSouza, and B. Gabrielli, *Oncogene*, 2008, **27**, 4261.
20. O. Flores, Z. Wang, K. E. Knudsen, and K. L. Burnstein, *Endocrinology*, 2010, **151**, 896.
21. T. Ma, B. A. Van Tine, Y. Wei, M. D. Garrett, D. Nelson, P. D. Adams, J. Wang, J. Qin, L. T. Chow, and J. W. Harper, *Gene Dev.*, 2000, **14**, 2298.
22. K. H. Oudah, M. A. A. Najm, N. Samir, R. A. T. Serya, and K. A. M. Abouzid, *Bioorg. Med. Chem.*, 2019, **92**, 103239.
23. S. Tadesse, E. C. Caldon, W. Tilley, and S. Wang, *J. Med. Chem.*, 2019, **62**, 4233.
24. P. C. Diao, W. Y. Lin, X. Jian, Y. H. Li, W. W. You, and P. L. Zhao, *Eur. J. Med. Chem.*, 2019, **179**, 197.
25. F. D. A. Walte, L. Sophie, M. Laurent, H. Libor, S. Miroslav, and K. Sung-Hou, *Eur. J. Biochem.*, 1997, **243**, 518.
26. D. Parry, T. Guzi, F. Shanahan, N. Davis, D. Prabhavalkar, D. Wiswell, W. Seghezzi, K. Paruch, M. P. Dwyer, and R. Doll, *Mol. Cancer Ther.*, 2010, **9**, 2344.
27. M. G. Brasca, N. Amboldi, D. Ballinari, A. Cameron, E. Casale, G. Cervi, M. Colombo, F. Colotta, V. Croci, and R. D'Alessio, *J. Med. Chem.*, 2009, **52**, 5152.

28. M. Reck, L. Horn, S. Novello, F. Barlesi, I. Albert, E. Juhász, D. Kowalski, G. Robinet, J. Cadranel, P. Bidoli, J. Chung, A. Fritsch, U. Drews, A. Wagner, and R. Govindan, *J. Thorac. Oncol.*, 2019, **14**, 701.
29. X. J. Chu, W. DePinto, D. Bartkovitz, S. S. So, B. T. Vu, K. Packman, C. Lukacs, Q. Ding, N. Jiang, and K. Wang, *J. Med. Chem.*, 2006, **49**, 6549.
30. D. R. Camidge, D. Smethurst, J. Growcott, N. C. Barrass, J. R. Foster, S. Febbraro, H. Swaisland, and A. Hughes, *Cancer Chemother. Pharmacol.*, 2007, **60**, 391.
31. M. K. Pasha, R. Jayaraman, V. P. Reddy, P. Yeo, E. Goh, A. Williams, K. C. Goh, and E. Kantharaj, *Drug Metab. Lett.*, 2012, **6**, 33.
32. A. Conroy, D. E. Stockett, D. Walker, M. R. Arkin, U. Hoch, J. A. Fox, and R. E. Hawtin, *Cancer Chemother. Pharmacol.*, 2009, **64**, 723.
33. D. A. Heathcote, H. Patel, S. H. Kroll, P. Hazel, M. Periyasamy, M. Alikian, S. K. Kanneganti, A. S. Jogalekar, B. Scheiper, and M. A. Barbazanges, *J. Med. Chem.*, 2010, **53**, 8508.
34. P. G. Wyatt, A. J. Woodhead, V. Berdini, J. A. Boulstridge, M. G. Carr, D. M. Cross, D. J. Davis, L. A. Devine, T. R. Early, and R. E. Feltell, *J. Med. Chem.*, 2008, **51**, 4986.
35. M. S. Squires, R. E. Feltell, N. G. Wallis, E. J. Lewis, D. M. Smith, D. M. Cross, J. F. Lyons, and N. T. Thompson, *Mol. Cancer Ther.*, 2009, **8**, 324.
36. D. Mahadevan, R. Plummer, M. Squires, D. Rensvold, S. Kurtin, C. Pretzinger, T. Dragovich, J. Adams, V. Lock, and D. A. Smith, *Ann. Oncol.*, 2011, **22**, 2137.
37. P. Pevarello, M. G. Brasca, R. Amici, P. Orsini, G. Traquandi, L. Corti, C. Piutti, P. Sansonna, M. Villa, and B. S. Pierce, *J. Med. Chem.*, 2004, **47**, 3367.
38. K. F. Byth, C. Geh, C. L. Forder, S. E. Oakes, and A. P. Thomas, *Mol. Cancer Ther.*, 2006, **5**, 655.
39. G. S. Mani, S. P. Shaik, Y. Tangella, S. Bale, C. Godugu, and A. Kamal, *Org. Biomol. Chem.*, 2017, **15**, 6780.
40. A. K. Bagdi, S. Santra, K. Monir, and A. Hajra, *Chem. Commun.*, 2015, **51**, 1555.
41. R. Goel, V. Luxami, and K. Paul, *Curr. Top. Med. Chem.*, 2016, **30**, 3590.
42. C. Hamdouchi, B. Zhong, J. Mendoza, E. Collins, C. Jaramillo, J. E. D. Diego, D. Robertson, C. D. Spencer, B. D. Anderson, S. A. Watkins, F. Zhang, and H. B. Brooks, *Bioorg. Med. Chem. Lett.*, 2005, **15**, 1943.
43. M. Anderson, J. F. Beattie, G. A. Breault, J. Breed, K. F. Byth, J. D. Culshaw, R. P. A. Ellston, S. Green, C. A. Minshull, R. A. Norman, R. A. Pauptit, J. Stanway, A. P. Thomas, and P. J. Jewsbury, *Bioorg. Med. Chem. Lett.*, 2003, **13**, 3021.
44. A. D. Patel, T. Y. Pasha, P. Lunagariya, U. Shah, T. Bambharoliya, and R. Tripathi, *ChemMedChem*, 2020, **15**, 1229.

45. U. Shah, S. Patel, M. Patel, and K. Gandhi, *Indian J. Chem.*, 2020, **59B**, 283.
46. A. Patel, K. Gandhi, S. Shah, D. Patel, S. Chhatbar, D. Shah, S. Patel, H. Patel, and T. Bambharoliya, *Curr. Comput. Aided Drug Des.*, 2022, **18**, 293.
47. U. Shah, A. Patel, S. Patel, M. Patel, A. Patel, S. Patel, S. Patel, R. Maheshwari, A. G. Mtewa, and K. Gandhi, *Curr. Med. Chem. Anticancer Agents*, 2022, **22**, 2063.
48. B. Bhimani, A. Patel, D. Shah, S. Patel, and T. Bambharoliya, *Indian J. Heterocycl. Chem.*, 2022, **32**, 455.
49. A. Shah, C. Patel, G. Parmar, A. Patel, and M. A. Jain, *Curr. Drug Ther.*, 2022, **17**, 96.
50. A. Patel, R. Vanecha, J. Patel, D. Patel, U. Shah, and T. Bambharoliya, *Mini-Rev. Med. Chem.*, 2022, **22**, 200.